SEMARAK ILMU PUBLISHING

Journal of Advanced Research in Micro and Nano Engineering

Journal homepage:
https://semarakilmu.com.my/journals/index.php/micro_nano_engineering/index
ISSN: 2756-8210

Development of Predictive Finite Element Models for Complete Contact Fretting Fatigue

Mohamad Haidir Maslan[1,*], Mohammad Aslam Sheikh[2], Nor Azazi Ngatiman[1], Nurul Amira Zainal[1], Saifudin Hafiz Yahaya[3]

[1] Department of Engineering Technology, Fakulti Teknologi dan Kejuruteraan Mekanikal, Universiti Teknikal Malaysia Melaka, Melaka, Malaysia
[2] School of Mechanical, Aerospace and Civil Engineering, University of Manchester, Manchester, United Kingdom
[3] Department of Engineering, Fakulti Teknologi dan Kejuruteraan Industri dan Pembuatan, Universiti Teknikal Malaysia Melaka, Melaka, Malaysia

ARTICLE INFO

Article history:
Received 14 October 2024
Received in revised form 20 November 2024
Accepted 26 December 2024
Available online 31 January 2025

Keywords:
Fretting fatigue; complete contact; finite element analysis; damage mechanics; fracture mechanics

ABSTRACT

Fretting fatigue is complex due to the interactions between contact mechanics and material fatigue properties. Predicting the total life in complete fretting fatigue is challenging due to different types of mechanical assemblies. This research develops a finite element model to predict this life, focusing on fatigue crack initiation and propagation in complete contact fretting fatigue. Crack initiation uses the Smith-Watson-Topper (SWT) criteria, considering wear and the material's elastic-plastic behavior. Crack propagation combines Linear Elastic Fracture Mechanics (LEFM), Elastic-Plastic Fracture Mechanics (EPFM), and Paris' law analysis. The SWT method with the addition of averaging shows good agreement with experimental data for crack initiation, possibly due to high singularities in complete contact. The combined LEFM and EPFM approach also aligns well for crack propagation. The estimated results had a 23% scatter compared to experimental data, demonstrating that combining damage and fracture mechanics provides a robust tool for predicting fretting fatigue life.

1. Introduction

Fretting fatigue occurs when two contact surfaces experience small oscillatory movements under load, leading to material damage and eventual failure. This type of fatigue is particularly dangerous because it often remains undetected until a catastrophic failure occurs [1,2]. Fretting fatigue involves complex interactions between contact mechanics, material properties, and environmental factors [3,4]. Unlike traditional fatigue, which mainly concerns cyclic loading, fretting fatigue includes the additional complexity of relative surface motion. This motion creates localized stress concentrations, significantly accelerating crack initiation and propagation [4-6].

Contact mechanics are crucial in fretting fatigue, as complete and incomplete contacts produce different stress profiles on the surface. Complete contact generates stress singularities at the contact

* *Corresponding author.*
E-mail address: haidir@utem.edu.my

https://doi.org/10.37934/armne.29.1.113

edges, leading to plastic deformation, microstructural changes, and residual stresses [7]. These stresses can worsen the fatigue process, making materials more prone to crack initiation and growth.

Moreover, the wear patterns differ between complete and incomplete contacts. Complete contact causes more uniform but potentially more severe wear due to higher edge stresses [8,9]. This wear further degrades material properties and structural integrity.

Despite extensive research, a gap remains in fully understanding the fretting fatigue mechanisms, particularly under complete contact conditions. Most existing models focus on incomplete contact and don't fully account for localized stress and material response. Understanding these factors in complete contact can greatly improve the safety and reliability of engineering systems. This journal aims to develop predictive finite element models that address these unique stress profiles and material responses in complete contact fretting fatigue scenarios.

This study proposes a two-step approach to model fretting fatigue. The first step predicts the location and number of cycles required for crack initiation using the Smith-Watson-Topper (SWT) method. The second step focuses on predicting crack propagation until failure. By integrating these two phases, our model aims to provide a comprehensive tool for forecasting fretting fatigue life and guiding the design and maintenance of components subjected to fretting conditions.

2. Methodology

2.1 Experimental Details

The finite element analysis is based on the experimental work of Fernando *et al.,* [10]. A general fretting fatigue test apparatus was utilized, comprising flat fretting bridge pads placed over a specimen with a rectangular cross section. The geometries of the pads and the specimen are illustrated in Figure 1. The material examined was a fully artificially-aged 4% copper aluminum alloy, while the fretting pads were made of BS S98 steel. The elastic properties of these materials are listed in Table 1.

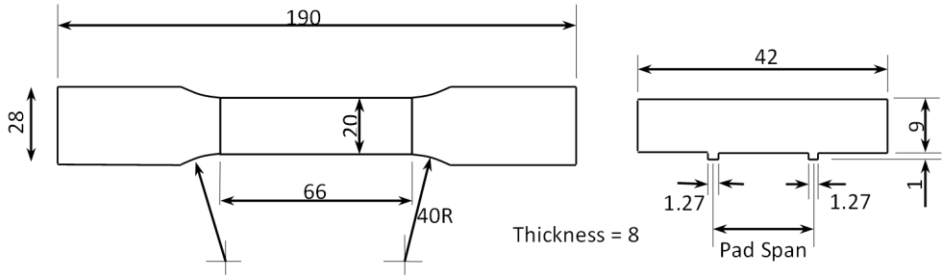

Fig. 1. Specimen and fretting pad (all dimensions in mm)

Table 1
Materials properties

Materials	Young modulus, E	Poisson ratio, v	Yield stress
BS L65	74.0 GPa	0.33	420 MPa
BS S98	210 GPa	0.29	1002 MPa

Three axial load amplitudes, 70 MPa, 100 MPa and 125 MPa with stress ratio, R=-1 were investigated, together with various values of normal load covering the range of 20 MPa to 120 MPa. The results of the experiments used in this analysis are summarised in Table 2. Potential Drop technique was used to get an estimation of the crack length during the fatigue test. The measurements were reported to be reliable for cracks longer than 0.1 mm.

Table 2
Materials properties

Axial stress (MPa)	Normal stress (MPa)	Crack initiation (number of cycles)	Crack initiation (% of life)	Fatigue life (number of cycles)
70	20	270,000	65.1	415,000
70	80	216,200	47.0	460,000
70	120	150,000	15.3	980,000
100	20	147,000	63.9	230,000
100	80	50,400	48.0	105,000
100	120	24,000	12.0	200,000
125	20	40,000	36.4	110,000
125	80	9,400	26.9	35,000
125	120	4,000	13.3	30,000

2.2 Numerical Modelling

Due to symmetry conditions, a quarter 2D finite element model has been used to represent the fretting fatigue tests, as shown in Figure 2. Since the specimen is 8 mm thick, plane strain elements are used in the analysis. Mesh is refined towards the contact region with a coarse mesh elsewhere, to reduce processing time. Matched meshes are used on the master and slave contact surfaces.

A Lagrange multiplier contact algorithm was used to strictly enforce the stick condition when the shear stress is less than the critical value according to the Coulomb friction law. Fernando *et al.,* [10] have suggested that a constant coefficient of friction (COF) value of 1 is representative for the tests studied here. The loading history is represented in Figure 3. In the first analysis step, a normal load, P is applied to the fretting pads. In the next step, the specimen is loaded by a cyclic fatigue load $\sigma(t)$ with a maximum value σ_{max} and a stress ratio, R of -1.

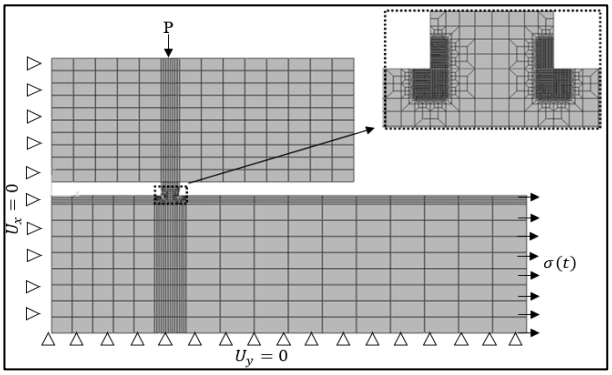

Fig. 2. Quarter finite element model

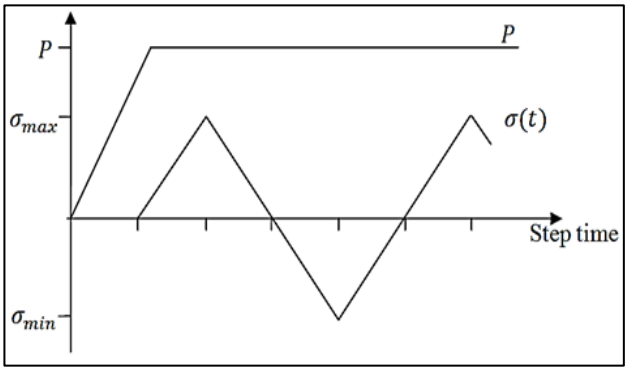

Fig. 3. Normal load and cyclic axial load history applied to the finite element model

2.2.1 Crack initiation

Crack initiation location and the number of cycles for initiation are determined by implementing SWT parameters on the critical plane where the product between the maximum stress and the total strain amplitude is maximum. Element centroidal stresses and strain ranges were calculated using the two-dimensional transformation (Mohr's circle) equations for stress and strain on every 5° intervals over a 180° range. The maximum normal stress (σ_{max}), and the corresponding strain range (Δε) are determined. These values together with fatigue properties as Table 3 are then employed in Eq. (1) to establish the SWT values and calculate the number of cycles for crack initiation.

$$SWT = \sigma_{max}\frac{\Delta\varepsilon}{2} = \frac{\sigma'^2_f}{E}\left(2N_f\right)^{2b} + \sigma'_f\varepsilon'_f\left(2N_f\right)^{b+c} \quad (1)$$

Table 3
Materials properties

σ'_f (MPa)	b	ε'_f	C
777	-0.1082	0.3041	-0.6478

The simulation considers the elastic-plastic behavior of the material and incorporates wear using a method closely following the technique implemented by Madge [9]. The wear formulation uses the Archard equation (Eq. (2)), which expresses wear at a specific point on the contacting surfaces.

$$\frac{h}{S} = kP \quad (2)$$

where h is the wear depth (m, k is the dimensional wear coefficient and P is the contact pressure (MPa). Based on Eq. (2), a numerical approach has been developed to simulate fretting wear. The modified Archard equation is then applied as follows:

$$\Delta h(x,t) = k\, p(x,t)\, \delta(x,t) \quad (3)$$

where $\Delta h(x,t)$, $p(x,t)$ and $\delta(x,t)$ are the incremental wear depth, contact pressure, and relative slip at point x and time t, respectively. Wear as Eq. (3) is simulated using an additional subroutine in Abaqus.

2.2.2 Crack propagation

This analysis utilized a conventional finite element procedure, modelling a stationary crack with varying lengths to determine the necessary stress intensity factors. An initial crack of 30 µm, located at the leading edge, was based on earlier predictions from crack initiation analysis and the experimental findings regarding crack length at nucleation. This initial crack, oriented according to the direction of maximum shear stress, matched the experimental results. The crack was then extended in small increments (20-50 µm) up to 0.5 mm, and larger increments of 0.25 mm beyond this point.

The crack was modelled in ABAQUS using an embedded line (referred to as a "seam" in ABAQUS). To improve the model's accuracy, mesh refinement was performed near the crack tip. A partitioning strategy was employed to generate the crack and facilitate the creation of a uniform focused mesh.

3. Results

3.1 Contact Stress

Contact stress during compressive and tensile loading is illustrated in Figure 4. The fretting pad exhibits rotational movement during cyclic loading in all cases. During compressive loading, the trailing edge lifts with no contact stress, while high pressure is generated at the leading edge as it is forced further into contact. This behaviour reverses during tensile loading.

The rotation of the fretting pad results from the combined effects of shear stress, which arises from slip, and the normal load applied to the pad. Shear stress generates a rotational moment in the pad, resisted by the moment created by the normal load. Consequently, rotation is more pronounced in specimens with low normal loads and axial stress values of 70 and 100 MPa. Rotation occurs in all

specimens except the one with an axial stress of 125 MPa, which produces higher slip; in these cases, the shear stress created by slip is sufficient to counteract the effect of the normal load.

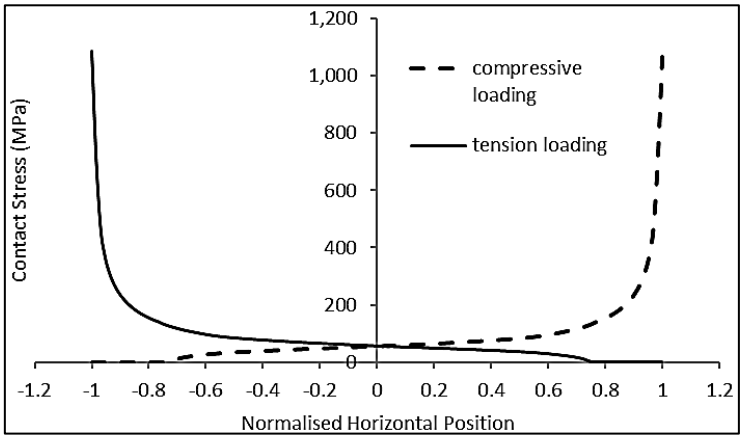

Fig. 4. Typical contact pressure distribution across the contact surface during compressive and tensile loading

3.2 Crack Initiation

The variation of the SWT parameter value across the contact surface is depicted in Figure 5. In all cases, the highest SWT parameter is found precisely at the leading edge, consistent with experimental observations where cracks typically occur at this location. Figure 6 illustrates the evolution of SWT parameter values over several applied load cycles across the contact surface. This analysis considers the elastic behaviour of the material and the wear occurring on the contact surface. The evolution of the SWT parameter is likely influenced by contact deformation due to repeated loading cycles. As the material undergoes more cycles, the contact surface deforms, potentially leading to changes in stress distribution and corresponding SWT values.

Crack nucleation predictions from the simulation are shown in Table 4. The number of cycles predicted for crack initiation is lower than the experimental data. Even when considering surface deformation caused by elastic-plastic behaviour and wear, the crack nucleation is predicted to occur within 10% of the cycles required to produce a 0.1 mm long crack experimentally. This finding differs significantly from Madge's [11] results, which showed that this method could accurately predict crack initiation for incomplete contact. This suggests that the method used for incomplete contact does not apply to complete contact. The discrepancy may be due to the high-stress gradient at the critical element caused by singularities. To account for the effect of singularities, an averaging technique is employed in this analysis.

The reason for such phenomena may be associated with the high stress gradient at the critical element due to singularities. In order to take the effect of singularities into account, an averaging technique is used in this analysis. This analysis uses averaging of SWT parameter, as proposed by Aroujo [12] over several elements on a certain area near the critical element to produce an average SWT parameter (SWT_{avg}).

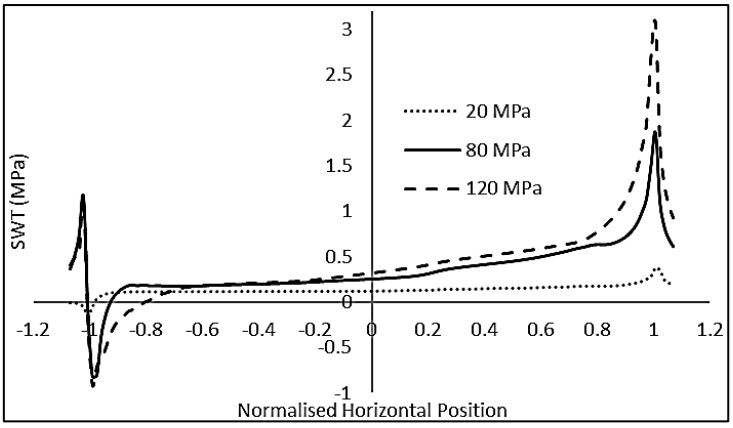

Fig. 5. Variation of SWT parameter across the contact surface for different applied normal loads for the axial stress of 100 MPa and a fixed COF value

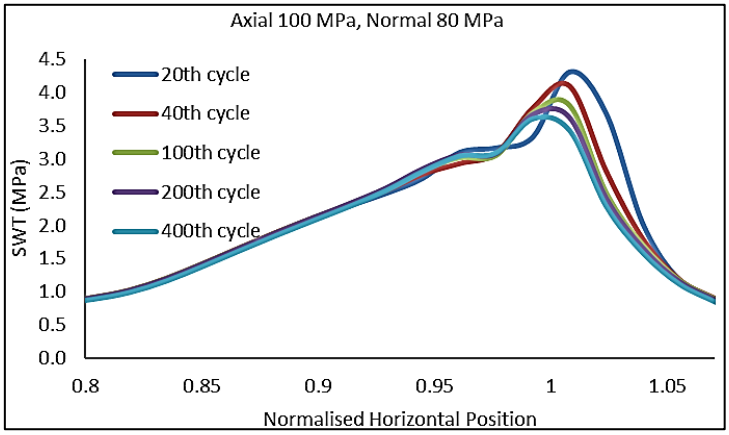

Fig. 6. Evolution of SWT parameter with applied load cycles across the contact surface

Table 4
Crack nucleation predictions by the elastic-plastic model including wear

Axial load (MPa)	Normal load (MPa)	Number of cycles to produce 0.1mm crack (experimental)	Crack nucleation prediction (SWT)	
			Number	% of exp.
70	20	270,000	3100	1.15
	80	380,000	430	0.11
	120	830,000	467	0.05
100	20	147,000	2850	1.94
	80	50,400	380	0.75
	120	24,000	314	1.31
125	20	40,000	970	2.43
	80	9,400	280	2.98
	120	4,000	170	4.25

Figure 7 shows the results obtained by applying several averaging sizes ranging from 30 µm to 70 µm and compared with the experimental data. Overall, it is clear that the averaged results give a better prediction when compared with the experimental data than the non-averaged ones. A detailed examination of each plot reveals that the prediction for specimen with normal stress of 20 MPa agrees well with the experimental results with an average size of 30 µm. For specimens with normal stress of 80 and 120 MPa and with applied axial stress of 100 and 120 MPa, the best fits with the experimental data are obtained with an averaging size of 50 µm. Specimens with normal stress

of 80 and 120 MPa and the applied axial stress of 70 MPa require a greater averaging size of 70 µm to produce good agreement with the experimental data.

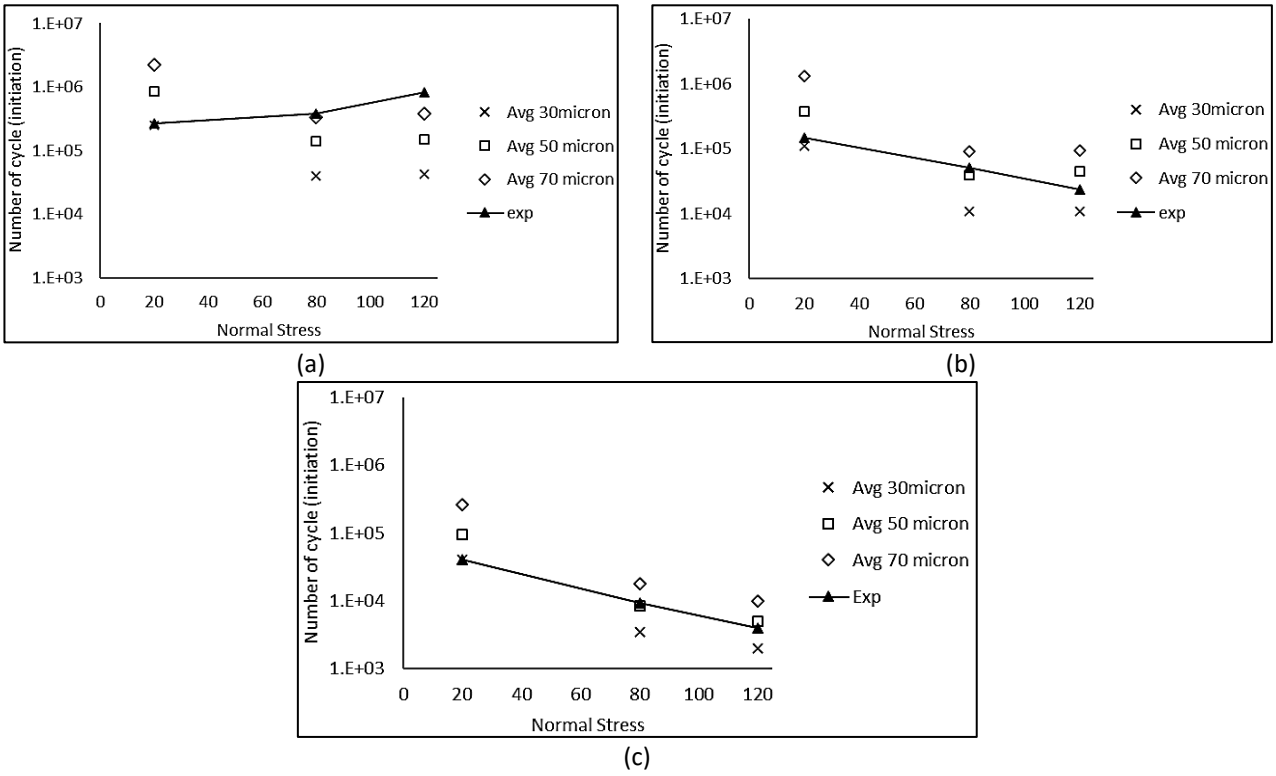

Fig. 7. Effect of averaging size on crack initiation prediction for specimens with applied stress (a) 70 MPa (b) 100 MPa (c) 125 MPa

These results agree with Aroujo [12], who suggests that the range of averaging dimension appears to be of a similar order of magnitude as the grain size. The averaging size for all the specimens is almost one or two times the grain size of the aluminium alloy (L65) used in this study [13]. Aroujo [12] also suggests that this averaging parameter may not be a true material constant but depends upon loading and some other factors. In this study, a similar trend is observed between pads rotation and the averaging size. As discussed before fretting pads rotation is pronounced for specimens with low normal loads. Specimens with normal load of 20 MPa are also found to be significantly affected by plastic deformation and wear as compared to other specimens. The material properties near the critical element may change due the plastic deformation and degradation due to wear. If taken into account in the SWT parameter, these changes in material properties may produce the same averaging size as other specimens.

For specimens with normal stress of 80 and 120 MPa, fretting pad rotation is more significant for high applied axial stress. Consequently, plastic deformation produced by this high stress due to pad rotation also seems to influence the results. However, a limited number of experimental results do not allow more conclusive evidence.

3.3 Crack Propagation

3.3.1 Crack path in complete contact fretting fatigue

In this study, two criteria, which have been shown to work well to determine crack growth direction, are used. These criteria are based on Maximum Tangential Stress (MTS) by Faanes [14] and Maximum Tangential Stress Range (ΔMTS) by Giner [15]. Faanes [14] used mathematical

formulations to determine stress intensity factors for mode I and mode II analyses. These values were then used to determine the stress field in front of the crack tip. Giner [15], on the other hand, analysed the problem with ABAQUS for a single pad complete contact. Figure 8 shows the results from the analysis. Overall, ΔMTS produced better predictions compared to MTS criterion, although both criteria assumed the crack to propagate in the direction of maximum tangential stress. However, MTS considers the stress field in front of the crack tip when the tangential stress is maximum which occurs when the applied axial stress is tensile. ΔMTS, on the other hand, considers the stress field over one complete cycle.

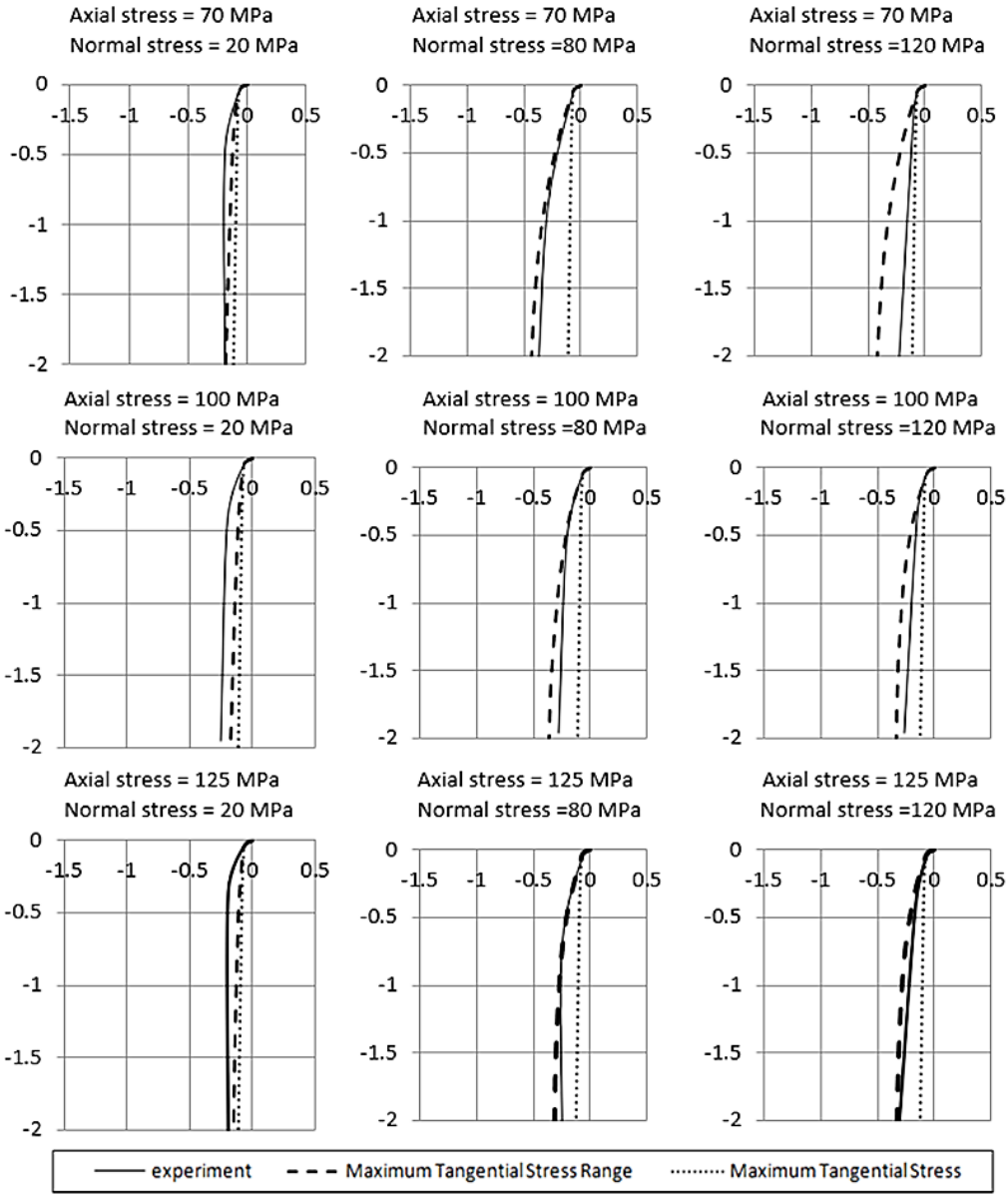

Fig. 8. Comparison of crack path observed in the experimental work and predicted by FEM using MTS and ΔMTS criteria

Contact stress at maximum tension and compression during the applied axial stress cycle can be observed previously in Figure 4. There is no contact stress at the surface near the leading edge in tensile loading. But the contact stress is very high at maximum applied compressive stress due to a small rotational movement of the fretting pad. In other words, during maximum tensile loading, the stress at the leading edge is almost like the specimen with only axial stress but without any contact

effect. This may be the reason why MTS crack is almost straight. Meanwhile, ΔMTS which considers the stress field for the whole cycle in the calculation can incorporate the multi axial effect in the prediction.

3.3.2 Crack propagation analysis

The predicted number of cycles from this approach are presented in Figures 9 to 11. Predicted number of cycles for crack propagation together with the predicted number of cycles for crack initiation, as obtained earlier then be compared with the experimental data.

In all cases, the predicted number of cycles is higher than the experimental results. In other words, it can be seen that the propagation from experimental work is slower than predicted. High plastic zone over crack length ratio as shown in Figure 12 can be the main reason for this difference. Plastic zone has been known to give the effect to slow down the rate as plastic deformation blunts the crack [16,17]. The small peak that occurs by the heterogeneous stress field near the surface also can cause retardation to slow down the crack [18-20].

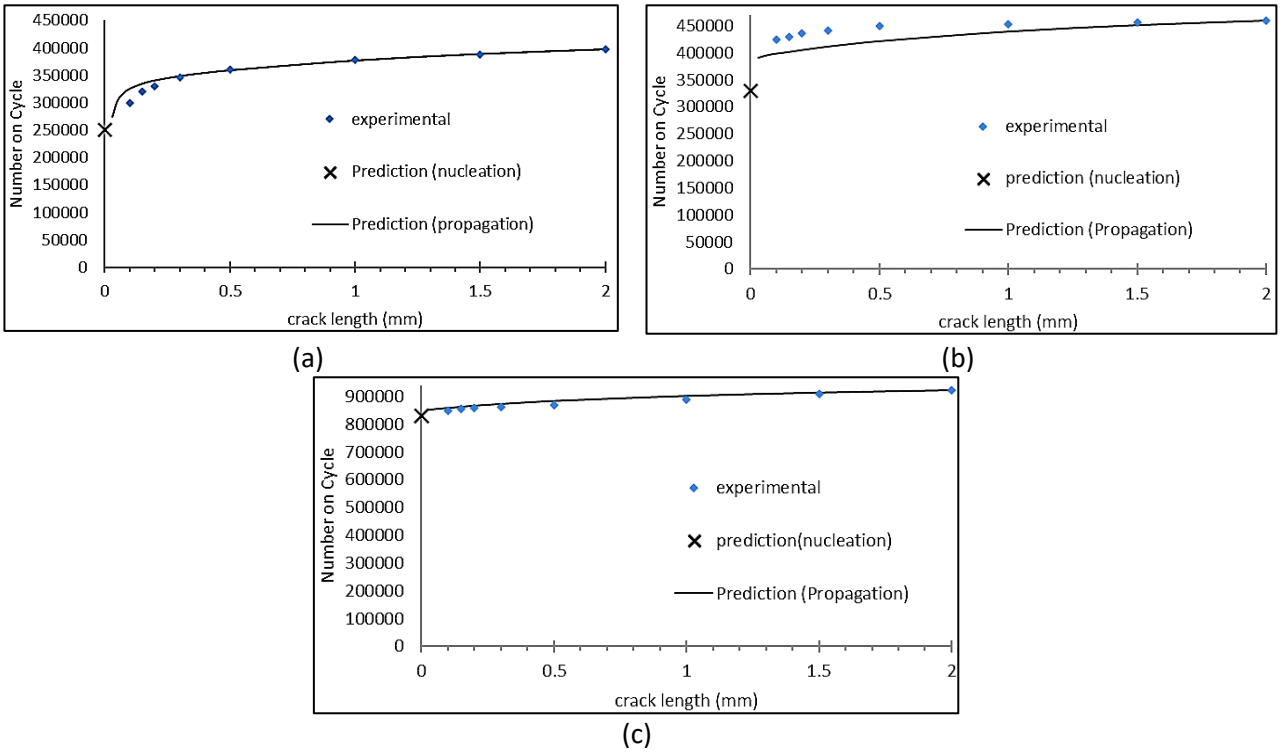

Fig. 9. Predicted number of cycles of crack propagation for specimens with applied axial stress of 70 MPa and normal loads (a) 20 MPa (b) 80 MPa (c) 120MPa

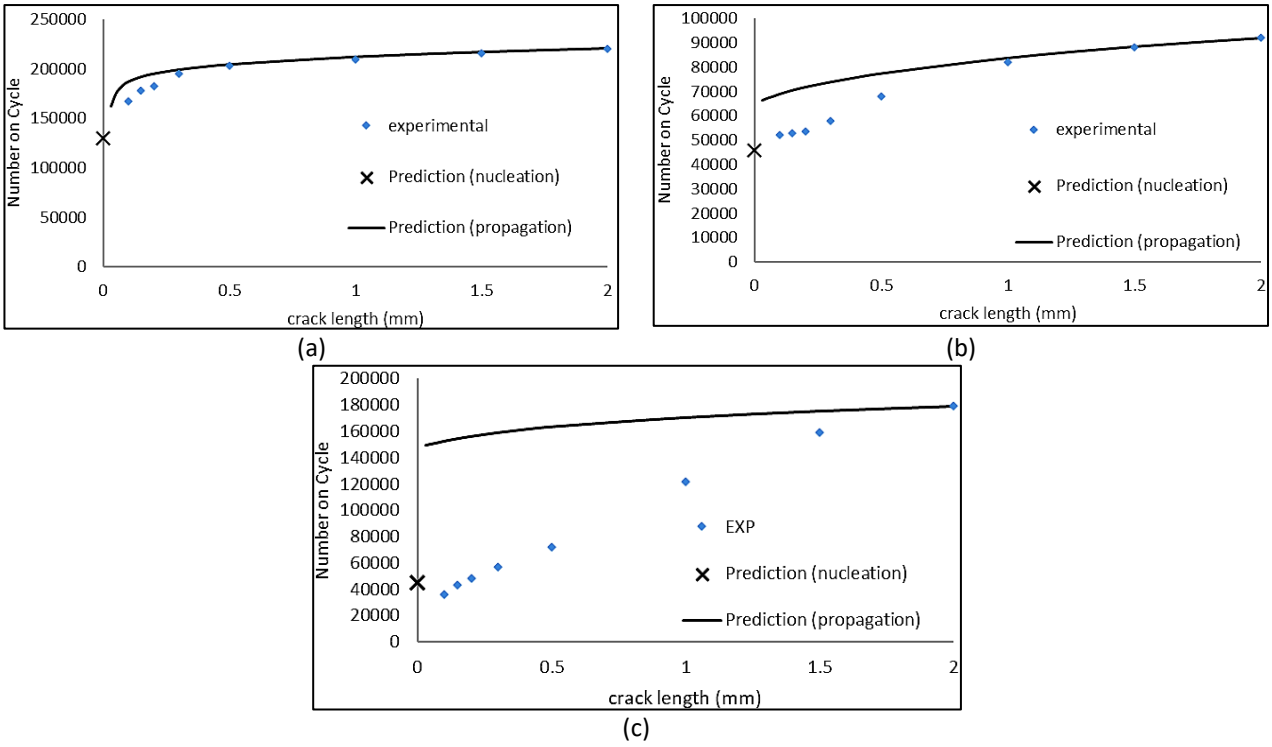

Fig. 10. Predicted number of cycles of crack propagation for specimens with applied axial stress of 100 MPa and normal loads (a) 20 MPa (b) 80 MPa (c) 120MPa

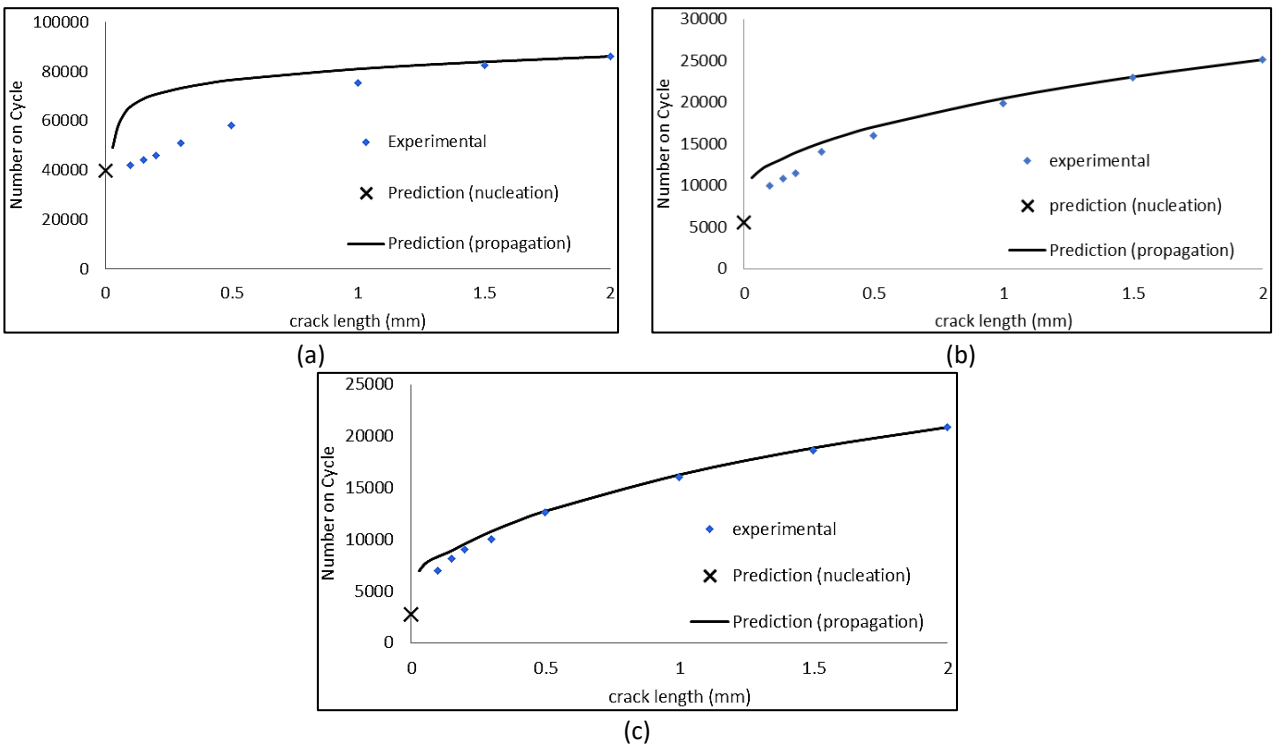

Fig. 11. Predicted number of cycles of crack propagation for specimens with applied axial stress of 125 MPa and normal loads (a) 20 MPa (b) 80 MPa (c) 120MPa

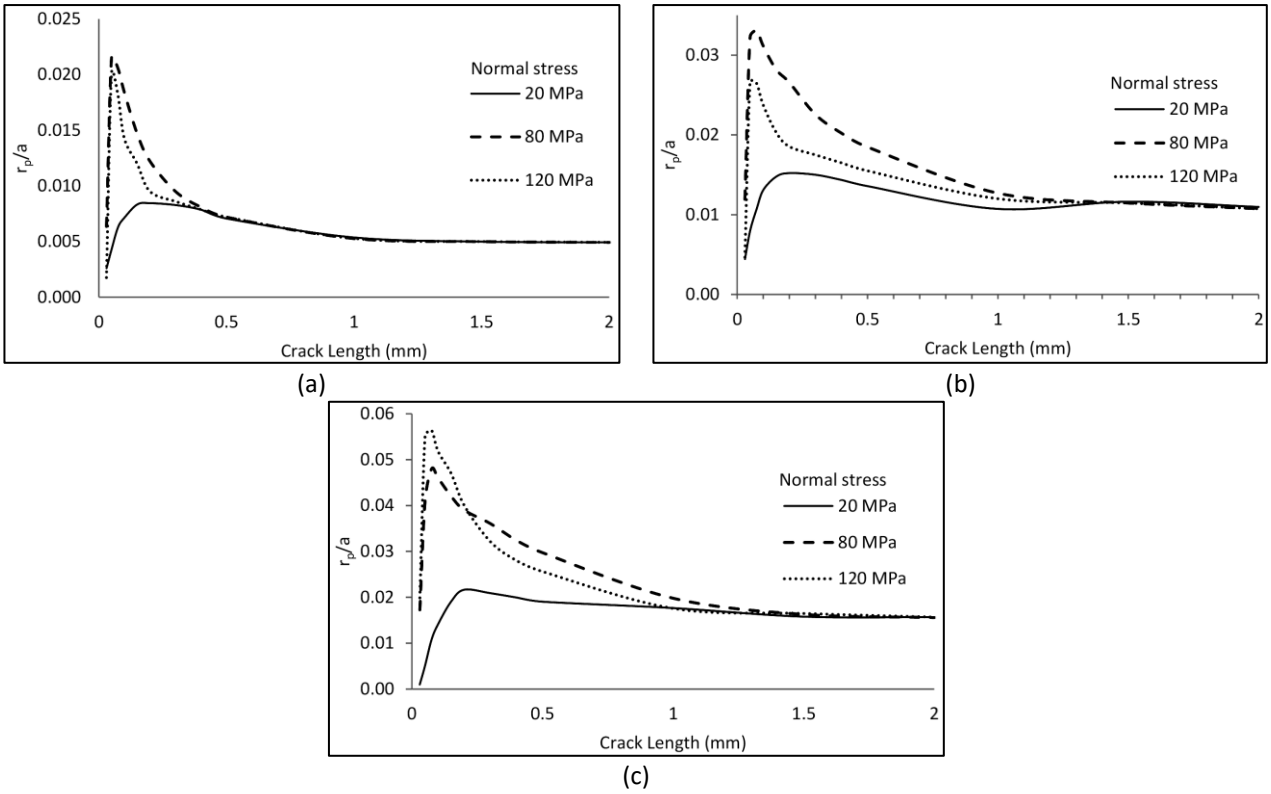

Fig. 12. Variation of plastic zone size (r_p) at the crack tip with crack length for different normal stress values and the applied axial stress (a) 70 MPa (b) 100 MPa (c) 125 MPa

3.4 Total Lifetime Prediction

Figure 13 shows the predicted total lifetimes and compared with experimental data. The estimated results are scattered within ±50% or with average of 23% of the experimental data. This clearly shows that the models developed here are capable of satisfactorily predicting lifetime in complete contact fretting fatigue.

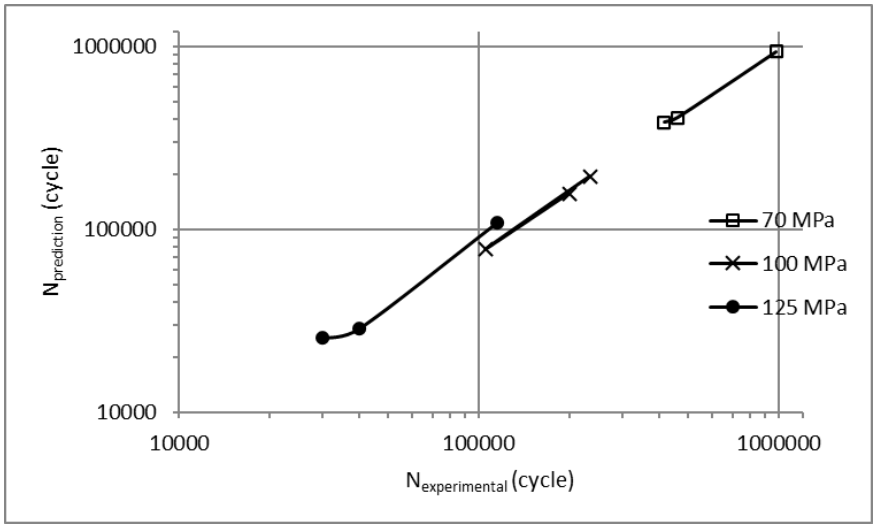

Fig. 13. Prediction of total fretting fatigue lifetimes and their comparison with the experimental data

4. Conclusions

The main goal of this project was to develop a reliable finite element model for predicting the total life in complete contact fretting fatigue. This involved two key aspects: fatigue crack initiation and fatigue crack propagation. These two techniques were studied separately and then combined for a comprehensive life prediction, shedding light on the interactions in complete contact scenarios. For crack initiation analysis, the strain-life multiaxial fatigue relationship was used. The Smith-Watson-Topper (SWT) criteria were chosen to predict crack initiation, with predictions aligning well with experimental observations where cracks typically occur at the leading edge.

Fatigue cycles caused micro-rotation of the fretting pad, intensifying edge singularities. With a stress ratio of R = -1, both edges were affected by strong singularities. This differentiation from incomplete contact explains why the predicted cycles for crack nucleation, despite improvements in elastic-plastic and wear models, are still within 10% of experimental results for a 0.1mm crack. This is due to the SWT parameter being influenced by steep stress gradients at the fretting pad edges. An averaging approach provided better predictions compared to experimental data. Observations showed that averaging several nodes around the critical element, with a size matching one to two times the grain sizes, improved accuracy. This averaging size depended on loading and other factors like wear and plastic deformation.

Crack propagation analysis was based on fracture mechanics theory. Initially, contact stress influenced crack growth, requiring multiaxial fatigue crack growth analysis. Under multiaxial stress states from fretting loads, cracks can change direction, making crack orientation and propagation crucial parameters. To determine the crack path in fretting fatigue, the maximum tangential stress range (ΔMTS) criterion was effective. Early-stage analysis showed a plastic zone to crack length ratio over 1/50, invalidating LEFM analysis. Therefore, a combined LEFM-EPFM model with Paris Equation analysis was used. EPFM analysis clarified the heterogeneous stress field's impact on stress intensity, showing that the large plastic zone in front of the crack tip retards crack propagation. This justified a different analysis for small crack propagation, which aligned well with experimental results after the early stage.

The proportion of fretting fatigue life spent in crack initiation and propagation varied between specimens. Combining crack initiation and propagation analysis was crucial for understanding fretting fatigue. The estimated results had a 23% scatter compared to experimental data, indicating that a combination of damage and fracture mechanics approaches provides a good estimation tool for predicting total fretting fatigue life.

Acknowledgement

Authors acknowledge Universiti Teknikal Malaysia Melaka and University of Manchester for supporting this study.

References

[1] Ozarde, Amit Prakash, Gene McNay, and Sachin Singh Gautam. "Fretting fatigue failures in internal combustion engine components." *SAE International Journal of Engines* 14, no. 2 (2021): 211-234. https://doi.org/10.4271/03-14-02-0013

[2] Farris, T. N., M. P. Szolwinski, and G. Harish. "Fretting in aerospace structures and materials." In *Fretting Fatigue: Current Technology and Practices*. ASTM International, 2000. https://doi.org/10.1520/STP14752S

[3] Croccolo, Dario, Massimiliano De Agostinis, Stefano Fini, Giorgio Olmi, Francesco Robusto, and Chiara Scapecchi. "Fretting fatigue in mechanical joints: a literature review." *Lubricants* 10, no. 4 (2022): 53. https://doi.org/10.3390/lubricants10040053

[4] Pinto, A. L., R. Talemi, and J. A. Araújo. "Fretting fatigue total life assessment including wear and a varying critical distance." *International Journal of Fatigue* 156 (2022): 106589. https://doi.org/10.1016/j.ijfatigue.2021.106589

[5] Bhatti, Nadeem Ali, and Magd Abdel Wahab. "Fretting fatigue crack nucleation: A review." *Tribology International* 121 (2018): 121-138. https://doi.org/10.1016/j.triboint.2018.01.029
[6] Araújo, J. A., F. C. Castro, I. M. Matos, and R. A. Cardoso. "Life prediction in multiaxial high cycle fretting fatigue." *International Journal of Fatigue* 134 (2020): 105504. https://doi.org/10.1016/j.ijfatigue.2020.105504
[7] Panico, Pierre, Thibaut Chaise, Marie-Christine Baietto, Nicolas Guillemot, and Cédric Poupon. "On the fretting fatigue crack nucleation of complete, almost complete and incomplete contacts using an asymptotic method." *International Journal of Solids and Structures* 233 (2021): 111209. https://doi.org/10.1016/j.ijsolstr.2021.111209
[8] Sunde, Steffen L., Bjørn Haugen, and Filippo Berto. "Experimental and numerical fretting fatigue using a new test fixture." *International Journal of Fatigue* 143 (2021): 106011. https://doi.org/10.1016/j.ijfatigue.2020.106011
[9] Argatov, Ivan, and Young Suck Chai. "Contact geometry adaptation in fretting wear: A constructive review." *Frontiers in Mechanical Engineering* 6 (2020): 51. https://doi.org/10.3389/fmech.2020.00051
[10] Fernando, U.S., Farrahi, G.H., Sheikh, M.A. "Fretting fatigue behaviour of BS L65 aluminium alloy", *Progress Report, SIRIUS. 1992*, University of Sheffield: Sheffield. https://doi.org/10.4028/www.scientific.net/AMM.467.431
[11] Madge, J. J., S. B. Leen, and P. H. Shipway. "A combined wear and crack nucleation–propagation methodology for fretting fatigue prediction." *International Journal of Fatigue* 30, no. 9 (2008): 1509-1528. https://doi.org/10.1016/j.ijfatigue.2008.01.002
[12] Araujo, J. A., and D. J. I. J. O. F. Nowell. "The effect of rapidly varying contact stress fields on fretting fatigue." *International Journal of Fatigue* 24, no. 7 (2002): 763-775. https://doi.org/10.1016/S0142-1123(01)00191-8
[13] Babu, S., GD Janaki Ram, P. V. Venkitakrishnan, G. Madhusudhan Reddy, and K. Prasad Rao. "Microstructure and mechanical properties of friction stir lap welded aluminum alloy AA2014." *Journal of Materials Science & Technology* 28, no. 5 (2012): 414-426. https://doi.org/10.1016/S1005-0302(12)60077-2
[14] Faanes, S. "Inclined cracks in fretting fatigue." *Engineering Fracture Mechanics* 52, no. 1 (1995): 71-82. https://doi.org/10.1016/0013-7944(94)00331-B
[15] Giner, Eugenio, Mohamad Sabsabi, Juan José Ródenas, and F. Javier Fuenmayor. "Direction of crack propagation in a complete contact fretting-fatigue problem." *International Journal of Fatigue* 58 (2014): 172-180. https://doi.org/10.1016/j.ijfatigue.2013.03.001
[16] Marco, Miguel, Diego Infante-Garcia, Jose Diaz-Alvarez, and Eugenio Giner. "Relevant factors affecting the direction of crack propagation in complete contact problems under fretting fatigue." *Tribology International* 131 (2019): 343-352. https://doi.org/10.1016/j.triboint.2018.10.048
[17] Nordin, Muhammad Haziq Iqmal Mohd, Khairum Hamzah, Nik Mohd Asri Nik Long, Najiyah Safwa Khashi'ie, Iskandar Waini, Nurul Amira Zainal, and Sayed Kushairi Sayed Nordin. "Stress Intensity Factors for Thermoelectric Bonded Materials Weakened by an Inclined Crack." *Journal of Advanced Research in Applied Mechanics* 113, no. 1 (2024): 52-62. https://doi.org/10.37934/aram.113.1.5262
[18] Iranpour, Mohammad, and Farid Taheri. "On the effect of stress intensity factor in evaluating the fatigue crack growth rate of aluminum alloy under the influence of compressive stress cycles." *International Journal of Fatigue* 43 (2012): 1-11. https://doi.org/10.1016/j.ijfatigue.2012.01.020
[19] Yang, B., and S. Mall. "Mechanics of two-stage crack growth in fretting fatigue." *Engineering Fracture Mechanics* 75, no. 6 (2008): 1507-1515. https://doi.org/10.1016/j.engfracmech.2007.06.009
[20] Venugopal, Arvinthan, Roslina Mohammad, and Md Fuad Shah Koslan. "Fatigue crack growth prediction on Su-30MKM horizontal stabilizer lug using static analysis." *Journal of Advanced Research in Applied Mechanics* 99, no. 1 (2022): 10-23.